

Osteophyte growth in early thumb carpometacarpal osteoarthritis

J.J. Crisco ^{† *}, A.M. Morton [†], D.C. Moore [†], L.G. Kahan [†], A.L. Ladd [§], A.-P.C. Weiss [†]

[†] Bioengineering Laboratory, Department of Orthopaedics, The Warren Alpert Medical School of Brown University and Rhode Island Hospital, 1 Hoppin Street, CORO West Suite 404, Providence, RI 02903, USA

[‡] Robert A. Chase Hand & Upper Limb Center, Department of Orthopaedic Surgery, Stanford University School of Medicine, Stanford, CA, USA

[§] Department of Orthopaedics, The Warren Alpert Medical School of Brown University/University Orthopedics, 2 Dudley Street, Suite 200, Providence, RI 02905, USA



ARTICLE INFO

Article history:

Received 11 October 2018

Accepted 3 May 2019

Keywords:

Thumb
Carpometacarpal
Osteophytes
Growth
Volume

SUMMARY

Objective: Osteophyte formation is a critical part of the degeneration of a joint with osteoarthritis (OA). While often qualitatively described, few studies have succeeded in quantifying osteophyte growth over time. Using computed tomography (CT) image data from a longitudinal, observational study of thumb carpometacarpal (CMC) OA, our aim was to quantify osteophyte growth volume and location over a three-year period in men and women.

Method: Ninety patients with early thumb OA were recruited and assessed at baseline, 1.5 years, and 3 years with CT imaging. Osteophyte volume and location on the trapezium and first metacarpal were determined using a library of 46 healthy subjects as a nonarthritic reference database.

Results: There was a significant increase in osteophyte volume for women and men over the three-year follow-up in the trapezium (86.8 mm^3 – 120.5 mm^3 and 165.1 mm^3 – 235.3 mm^3 , means respectively) and in the proximal metacarpal (63 mm^3 – 80.4 mm^3 , and 115.8 mm^3 – 161.7 mm^3 , respectively). The location of osteophyte initiation and growth was consistent across subjects and was located in non-opposing regions on the trapezium and first metacarpal. Osteophyte growth occurred about the radial and ulnar margins of the trapezial facet, while on the proximal metacarpal, growth occurred principally about the volar and dorsal margins of the facet.

Conclusion: Osteophyte growth occurred in early thumb osteoarthritis over three years. Growth was localized in specific, non-opposing regions on the trapezium and metacarpal, raising intriguing questions about the triggers for their formation, whether the mechanisms are mechanical, biological or a combination of both.

© 2019 Osteoarthritis Research Society International. Published by Elsevier Ltd. All rights reserved.

Introduction

Osteophytes are a sign of advancing joint degeneration in thumb carpometacarpal (CMC) osteoarthritis (OA), appearing radiographically with changes in joint space width and subchondral sclerosis^{1–3}. Osteophytes may be an important clinical metric of OA disease progression. Osteophytes have been shown to better predict knee pain than joint space narrowing, which is currently the only validated measure of osteoarthritis disease progression⁴. Similarly, in a study of patients with hip osteoarthritis, patients

who had radiographic evidence of OA but were pain-free had no broad signal changes in bone detected by MRI, while in a second group with persistent pain broad signal changes could be detected⁵. The authors proposed an association between bone signal changes on MRI and joint pain in the progression of hip OA⁵. Other studies have corroborated the association of pain with OA progression, as assessed by bony changes^{6–8}, suggesting the pathophysiology of OA progression and joint pain may be due primarily to bony changes⁹. A recent study by Kroon *et al.* found that thumb pain was more strongly linked to osteophyte formation than to soft tissue inflammation, leading the authors to speculate that thumb OA may be a phenotype distinct from finger OA⁶.

Typically described as bony outgrowths, osteophytes are in fact osteochondral exostoses formed by cells in activated periosteum and/or synovium at the joint margins, which then proliferate, differentiate into chondrocytes, hypertrophy, and mineralize via

* Address correspondence and reprint requests to: J.J. Crisco, Bioengineering Laboratory, Department of Orthopaedics, The Warren Alpert Medical School of Brown University and Rhode Island Hospital, 1 Hoppin Street, CORO West Suite 404, Providence, RI 02903, USA.

E-mail address: joseph_crisco@brown.edu (J.J. Crisco).

endochondral ossification^{10–12}. Morphologically, mature osteophytes contain trabecular bone and marrow that is contiguous with the pre-existing subchondral bone, and they are capped with fibrocartilage^{11,13}. Altered joint mechanics^{14–16} and aberrant biochemical signaling^{17,18} have each been proposed as initial triggers, however, it is likely both are involved. Osteophytes also alter joint surface area and shape, with implications of reducing articular contact stress at the joint due to increased surface area and motion at the joint due to impingement of the protruding osteophytes^{19–21}.

Osteophytes reportedly form in a characteristic pattern in thumb CMC OA, which was initially described by North and Rutledge²² as part of an anatomic study of joint shape and trapeziometacarpal degeneration. Analyzing explanted trapezia and metacarpals from 67 embalmed cadavers, they noted that osteophyte formation was earliest and “most severe” on the radial and ulnar margins of the trapezial articular facet, while metacarpal osteophytes appeared later and were most typically found on the dorsal and volar margins of the metacarpal facet. They depicted trapezial osteophytes as initially appearing at Eaton/Littler¹ Stage II, growing in size and scope to eventually encircle the articular surface by Stage IV. Their description of metacarpal osteophytes was less detailed, noting only that they did not occur until Eaton/Littler Stage IV, late in the disease process. Subsequent authors have echoed aspects of North and Rutledge's findings^{3,23,24}, with some suggesting that there may be other patterns of degeneration²⁴.

North and Rutledge's²² work was important because it largely formed the basis for our current understanding of osteophyte evolution in thumb CMC OA. However, it is limited in that the study design was cross-sectional (of necessity) and the descriptions of osteophyte growth results were qualitative and generalized. It would be a significant advance to have longitudinal quantitative data on osteophyte size and location from patients repeatedly sampled as their joints deteriorated and their OA progressed. Moreover, North and Rutledge did not stratify their findings by sex, despite the fact that thumb CMC OA is substantially more prevalent in women than men^{25,26}. It would be interesting to know if there were sex-related differences in the pattern and/or rate of osteophyte development. A more nuanced understanding of osteophyte growth and morphology should provide insight into their origin and role in the pathogenesis of thumb CMC OA.

The specific aims of this study were to quantify the volume and location of periarticular thumb CMC osteophytes as they emerge and grow during early OA development (i.e., in the first three years after presentation), and to determine if osteophyte volume (OP) differs between women and men. To accomplish these aims we utilized data from an ongoing longitudinal, computed tomography (CT) image-based observational study of thumb CMC biomechanics and OA progression, in which thumb kinematics and CMC joint pathology were serially evaluated at the time of study enrollment (time 0), and at 1.5-year follow-up intervals. We hypothesized that there would be significant osteophyte growth over the three-year follow-up period and that volume growth would be proportionally greater in women than in men.

Methods

Study subjects

After obtaining IRB approvals at Rhode Island Hospital and at Stanford University, 90 patients with early thumb CMC OA (early OA) and 46 healthy volunteers (non-OA) (Table 1) were recruited, consented, and enrolled into a large observational study on the role of biomechanics in thumb CMC OA progression (R01AR059185)^{27–36}. The early OA cohort were patients who presented with basilar thumb pain and no or minimal radiographic

Table 1

Baseline cohort demographics (mean \pm SD) and physical examination (positive tenderness to palpation (TTP), positive grind test (GT)), reported as a percentage (%) within each cohort and sex. The values listed for the non-OA are those of the healthy reference library

Cohort	Sex	n	Age (yrs.)	BMI	TTP (%)	GT (%)
non-OA	Women	25	41.9 \pm 17.5	28.1 \pm 7.1	0	0
	Men	21	40.3 \pm 19.0	25.2 \pm 3.7	0	0
OA	Women	47	53.4 \pm 5.9	25.9 \pm 5.8	62	17
	Men	43	60.3 \pm 7.3	28.1 \pm 4.3	70	40

changes (primarily modified Eaton Stage 0/1)³. Hand-directed histories and physical exams were performed by board certified orthopedic hand surgeons, which included measurements of body mass index (BMI), tenderness to palpation (TTP) and the grind test (GT). Non-OA subjects were eligible if they had no history of thumb pain or radiographic evidence of CMC OA. Exclusion criteria for both cohorts included pre-existing conditions that could influence CMC joint morphology or function (e.g., traumatic injury, inflammatory arthritis, hand or thumb surgery, etc.). In the early OA cohort, examinations were scheduled at enrollment (baseline), and at 1.5 and 3-year follow-up visits. The trapezia (TPM) and first metacarpals (MC1) of the non-OA subjects were used as a reference library to calculate osteophyte bone volumes described below.

At each examination, posteroanterior, lateral, Robert's, and stress view radiographs were acquired of the thumb. OA disease progression was determined by experienced hand surgeons (one at each study site) using a modified version of the 1987 Eaton-Glickel¹² classification in which early-stage disease (Eaton I) was refined, subluxation was eliminated as a measure of progressive radiographic deterioration, and all four available radiographic views were included³. The modified Eaton classification addresses mild disease by designating normal contour and joint space as stage 0, and minimal joint findings as stage 1. Consistent with the Eaton-Glickel criteria, “joint debris” was used to define stages two and 3 (<2 mm and >2 mm, respectively), while stage four in the modified classification includes severe TMC disease plus scaphotrapezoid and/or scaphotrapezial involvement, not just scaphotrapezial disease. The modified Eaton classification was reported to have a slightly higher ICC (0.83) amongst reviewers than the Eaton-Glickel classification (0.73)³.

CT imaging

At each exam, the wrists and thumbs of the affected hands of the early OA subjects and the dominant hands of the non-OA subjects were CT-scanned in a braced neutral position (Rolyan[®] Original, Patterson Medical, Bolingbrook, IL) and in 11 additional range-of-motion or task-related positions^{27,28,31,37}. Only CT images from the braced neutral scans were analyzed in this study. The scans were acquired with a 16-slice clinical scanner (GE LightSpeed 16, GE Medical, Milwaukee, WI) at tube settings for the neutral scan of 80 kVp and 80 mA. The resulting 3-D volume images had a resolution of 0.39 mm \times 0.39 mm \times 0.625 mm. The mean effective radiation exposure for each 12-scan CT imaging session was 0.323 mSv, which is equivalent to less than two months of naturally occurring background radiation (3 mSv/year)³⁸.

CT imaging processing and data analysis

Digital bone models of the outer cortical surfaces of the trapezia (TPM) and first metacarpals (MC1) were generated from the CT image volume via semi-automated segmentation with minimal smoothing (smoothing factor 0.030) (Mimics v12-20, Materialise,

Leuven, Belgium). Models of the trapezium (OA_{TPM}) and first metacarpal (OA_{MC1} , Fig. 1(A)) bones were generated from the enrollment (time 0), year 1.5, and year 3 follow-up CT scans for the early OA cohort, and from the enrollment (time 0) CT scan for the non-OA cohort.

OPs for the trapezium (OP_{TPM}) and first metacarpal (OP_{MC1} , Fig. 1(C)) were defined by intersecting (Boolean subtraction) the reference bone models and the early OA bone models at each time point. Specifically, the reference trapezium and first metacarpal models were selected for each early OA patient via least squares superimposition (rotation, translation, and scaling)³⁹ of bone models from the non-OA cohort to the time 0 bone models from the early OA cohort, with local dysmorphologies excluded to optimize alignment of the overall bone shapes^{40–42}. Each baseline early OA bone was fit with all 46 of the corresponding non-OA bones (trapezium and MC1) and the non-OA bone that yielded the smallest dissimilarity measure was selected as the reference bone (C^k_{TPM} and C^i_{MC1} , Fig. 1(B)). A reference library of bone models was used because we did not want to assume that the time 0 early OA bones were pathology free and we did not have contralateral CT images to use as a healthy reference⁴³. Rigid registration to each time 0 bone model was performed for all follow-up time points (Geomagic Wrap[®] 2017, 3D Systems, SC, USA). Boolean subtraction was used to generate closed surface models of the portions of the early OA bones that fell outside of the reference bone models. The closed surface models were truncated to limit analysis to the margins of the articular surfaces. The trapezial models were truncated with a cross-sectional plane (S_{TPM} , Fig. 1(B)) that was located at the geometric centroid of the trapezium and aligned with the trapezial coordinate system, whose origin was located at the inflection point of the articular surface³⁴. The MC1 models were truncated similarly, with a cross-sectional plane (S_{MC1} , Fig. 1(B)) offset from the MC1 coordinate system by the same distance as the corresponding trapezial centroid to coordinate system. To assess variations in bone shape that could potentially generate “false osteophytes” (e.g., an

unusual bony prominence), this same process of registration and Boolean subtraction was used on each of the non-OA bone models.

OP was computed by integrating⁴⁴ the non-intersecting volumes (OP_{TPM} and OP_{MC1} , Fig. 1(C)). To account for the greater bone size in men than in women, the OPs of the trapezium ($TPM OP_{vol,norm}$) and the proximal first metacarpal ($MC1 OP_{vol,norm}$) were normalized by the subject's total bone volumes at each time point and reported as a percentage (%) of total bone volume. To identify locations of differential osteophyte growth around the perimeter of the articular surface, the osteophyte growth models were divided into 72 five-degree (5°) arc sections (S^θ , Fig. 1(C)) and the volume of each section was calculated separately (OP^θ_{TPM} and OP^θ_{MC1} , Fig. 1(D)). To describe the locations of osteophyte growth, the sectional OPs were normalized by total bone volume and computed as a function of angular direction, where the key directions of 0° , 90° , 180° , 270° correspond to volar, radial, dorsal, and ulnar, respectively, based upon the trapezial and MC1 coordinate systems³⁴. Normalized growth locations were pooled for women and men as differences in the shape of the TPM and MC1, other than size, have not been reported⁴⁵. The computed non-intersecting volumes of the non-OA cohort are provided for descriptive comparisons with the OP and locations for the early OA cohort.

Statistical analysis

This study is a secondary analysis of data collected for an ongoing, longitudinal, CT image-based observational study designed to identify the biomechanical predictors of thumb CMC OA initiation and progression (R01AR059185)^{27–36}. Differences in total bone volume, OP, normalized OP, and CMC OA radiographic progression were evaluated with mixed models that included random intercepts for subjects and fixed effects for time (modeled as a categorical variable with baseline, year 1.5, and year three as levels), sex (modeled as a dichotomous variable with male and female as levels), and the two-way time \times sex interaction (Proc

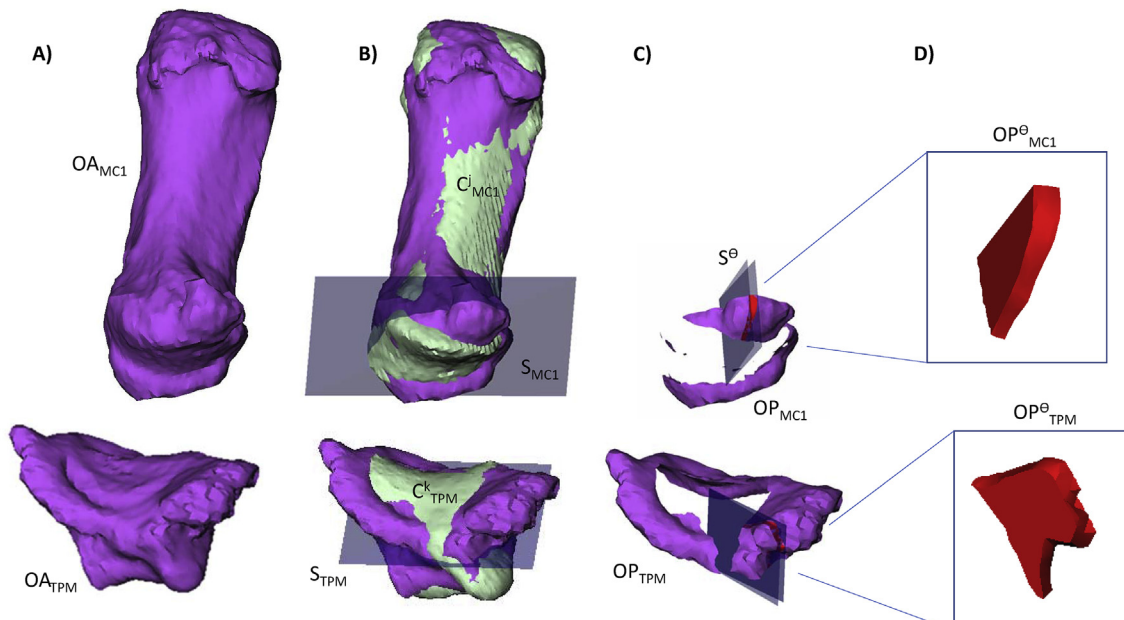


Fig. 1. Schematic of the algorithm for computing osteophyte growth volume and growth locations. Bone models of the first metacarpal (OA_{MC1}) and trapezium (OA_{TPM}) for each patient at baseline (A) were fit with the entire library of non-OA bones. The non-OA bones with the lowest dissimilarity measures were identified as the patient's reference bones (C^k_{TPM} and C^i_{MC1} , B). Boolean subtraction was applied and the resulting volume was trimmed by cross-sectional planes (S_{TPM} and S_{MC1} , B) to generate the models of CMC osteophytes for the MC1 (OP_{MC1}) and for the TPM (OP_{TPM}) (C). To compute osteophyte volume (OP) and growth by location, the osteophyte models were sectioned at intervals of 5° (S^θ , C) about the CMC (OP^θ_{MC1} and OP^θ_{TPM} , D).

GLIMMIX in SAS version 9.4, SAS Institute Inc., Cary, NC). Mixed models were chosen as they allow appropriate handling of data structures associated with repeated measurements and maximize the information from subjects with missing observations. To satisfy the assumption of normality, bone volume, OP, and normalized OP were logarithmically transformed after examination of their distributions and model residuals. Classical sandwich estimators were used to protect against model misspecification. The Holm test was used for multiple comparisons, maintaining a 2-tailed familywise alpha at 0.05. Adjusted p-values and model-based means and 95% confidence intervals (CIs) are reported. Curves of normalized (as a percent of total bone volume) 5° sectional osteophyte volume are plotted as a function of location about the joint circumference and reported with descriptive statistics (median, 25th percentile, and 75th percentile) at each time point.

Results

CMC OA progression was demonstrated radiographically, as the modified Eaton staging increased by approximately 8/10ths of a stage in women and men over the three-year study period (Table II, $P < 0.0001$ for both).

From baseline (time 0) to the three-year follow-up time point, mean TPM total bone volume increased by approximately 4% for men and women ($P < 0.0001$ for both) (Fig. 2(B), Table III). Over this same three-year period there were also significant but smaller increases in MC1 total bone volume (1% in women and 3% in men; $P = 0.02$ and $P < 0.0001$, respectively) (Fig. 2(A)). Total bone volume of the TPM and MC1 remained significantly larger in men than women ($P < 0.0001$, for both).

The mean volume of osteophytes rimming the trapezial CMC facet at baseline was 86.8 mm³ in women (4.9% of total bone volume) and 165.1 mm³ in men (6% of total bone volume) (Fig. 2(D), Table IV). Similarly, mean OP around the CMC facet of the MC1 was 63 mm³ in women (1% of total bone volume) and 116 mm³ in men (1.7% of total bone volume) at baseline (Fig. 2(C), Table IV). By the three-year follow-up, mean TPM OP increased significantly in women and men, to 120.5 mm³ and 235 mm³, respectively ($P < 0.0001$ for both) (Fig. 2(D), Table IV). MC1 mean OP also increased significantly in men and women, to 80.4 mm³ and 161.7 mm³, respectively, at the three-year follow-up ($P = 0.008$ and $P = 0.0005$, respectively) (Fig. 2(C), Table IV). At the three-year follow up, OP for the TPM and MC1 remained significantly larger in men than women ($P < 0.0001$ and $P = 0.0007$, respectively).

After normalizing by total bone volume, OPs remained significantly greater at the three-year follow-up than at baseline in women and men for the TPM and MC1 (TPM: $P < 0.0001$ for women and men, MC1: $P = 0.01$ and $P = 0.0009$, respectively) (Fig. 3). While the size of the OPs as a percentage of total bone volume was consistently larger in men than in women throughout the study, these differences were not statistically significant for either the TPM or MC1 at the three-year follow-up ($P = 0.12$ and $P = 0.49$).

Osteophytes formed and grew in consistent, non-opposing patterns about the TPM and MC1 (Fig. 4). Osteophyte formation was greatest on the radial and ulnar margins of the trapezial articular facet throughout the three-year observation period of the study (Fig. 4(B)), and it was greatest on the dorsal and volar (beak) margins of the MC1 articular facet (Fig. 4(A)). There was minimal osteophyte formation on the volar and dorsal margins of the TPM and minimal osteophyte formation on the radial and ulnar margins of the MC1 over the three-year course of the study. The minimal OPs on these margins were comparable in magnitude to the normal variations in the bone shape of the non-OA subjects at these same margins.

Discussion

In this study, osteophyte growth at the CMC joint in patients with early thumb CMC osteoarthritis was quantified using serial CT images acquired as part of a longitudinal study of CMC biomechanics and OA progression. Over the three-year observation period, significant osteophyte growth occurred. OP was greater in men than women, which was expected given that, on average, men have larger carpal bones than women⁴⁶. After normalizing for bone size, we did expect osteophyte growth to be greater in women than men, given the higher prevalence of thumb OA in women. However, we found no statistical sex-related differences in OP. On the contrary, the normalized OPs tended to be consistently greater in men (Fig. 3(A) and (B)).

Our most interesting finding was the pattern of osteophyte growth. In our early OA patients, osteophytes formed and grew in highly localized non-opposing regions on each bone: on the ulnar and radial margins of the trapezial articular facet, and on the dorsal and volar margins of the MC1 facet. Growth locations did not differ between women and men. These findings are consistent with those described by North and Rutledge²². In the cadavers they identified as having Eaton Stage II disease, which is relatively early-stage, North and Rutledge described osteophyte formation on the radial and ulnar margins of the trapezium. With more advanced degeneration they depicted osteophytes expanding to encircle the trapezial facet. Our patients were recruited into the study at modified Eaton Stage 0/1, and by year three had, on average, not yet advanced to the point where their osteophyte growth encircled the facet. Osteophyte formation on the volar and dorsal aspect of the trapezium was minimal – essentially comparable to that in the non-OA subjects (Fig. 4) – suggesting they had not reached the level of pathology of North and Rutledge's Stage III trapezia. It is reassuring that the same general osteophyte patterning was obtained with two different experimental designs: North and Rutledge's²² cross-sectional analysis of cadaver specimens and our longitudinal study.

Our results are also generally consistent with those of Buckland-Wright et al.⁴⁷, who radiographically studied osteophyte progression in patients with hand OA. They found that osteophytes at the thumb CMC joints were the largest compared to those of any other joint in the hand. Additionally, they found a high prevalence

Table II
Modified Eaton radiographic classification³ at baseline and each follow-up exam, reported as a percentage (%) within each cohort, sex and time point. The values listed for the non-OA are those of the healthy reference library

	Women						Men							
	0	1	2	3	4	mean	n	0	1	2	3	4	mean	n
Non-OA	84	16	0	0	0	0.16	25	95	5	0	0	0	0.05	21
OA 0 yr	38	62	0	0	0	0.62	47	19	79	2	0	0	0.84	43
OA 1.5 yr	29	40	26	5	0	1.07	42	7	43	40	10	0	1.52	42
OA 3 yr	17	45	19	17	2	1.43	42	15	28	33	23	0	1.64	39

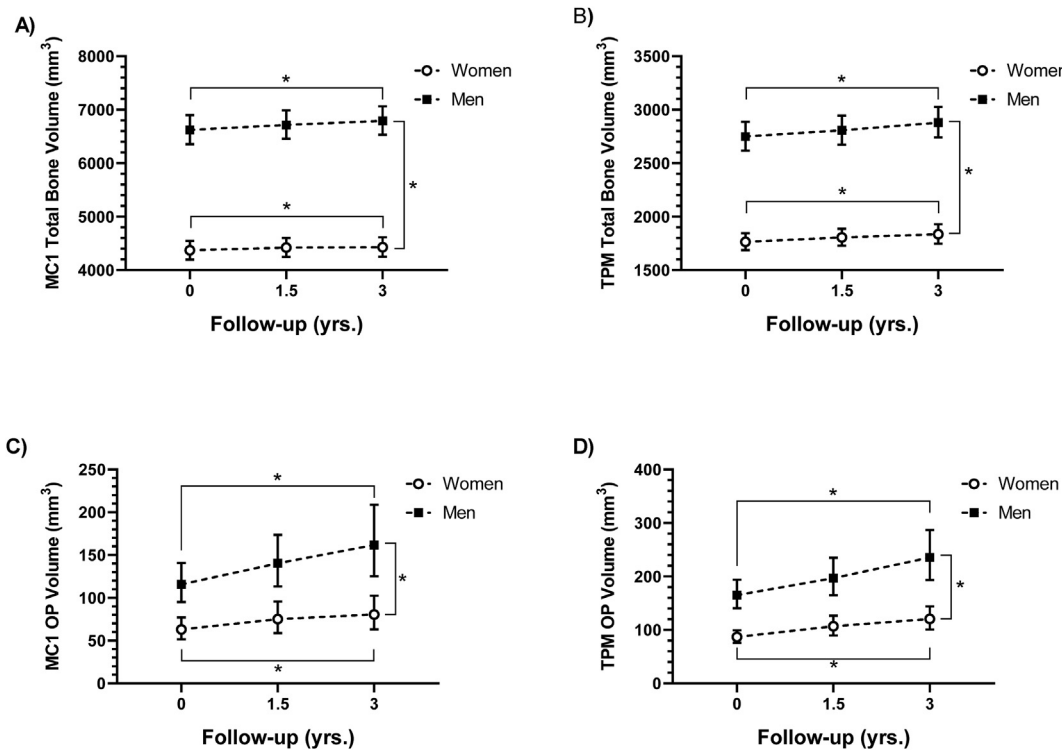


Fig. 2. Total bone volume and osteophyte volume (OP) of the first metacarpal (MC1) (A and C) and the trapezium (TPM) (B and D) significantly increased over the three-year follow-up in women and men. At the three-year follow-up, total bone volume and OP were significantly larger in men than in women. Model-based means and with their 95% confidence intervals (CIs) are plotted.

Table III

Minimum, maximum, median, 25th percentile, and 75th percentile of total bone volumes (mm³) of the trapezium (TPM) and first metacarpal (MC1). The values listed for the non-OA are those of the healthy reference library

Women						Men						
TPM	min	max	median	25 th %	75 th %	n	min	max	median	25 th %	75 th %	n
non-OA	1,230.7	2,682.1	1753.4	1,332.1	2,207.9	25	1775.8	3,500.6	2,472.4	1914.5	3,013.1	21
OA 0 yr	1,219.8	2,549.2	1822.6	1,457.0	2,115.9	47	1942.8	3,944.0	2,829.3	2,243.8	3,328.7	43
OA 1.5 yr	1,328.2	2,554.4	1845.9	1,475.8	2,145.1	42	1986.5	3,672.5	2,892.9	2,317.0	3,314.6	42
OA 3 yr	1,367.1	2,708.1	1888.4	1,488.3	2,213.0	42	1998.5	3,772.4	2,921.8	2,337.6	3,405.9	39
MC1	min	max	median	25 th %	75 th %	n	min	max	median	25 th %	75 th %	N
non-OA	2,642.4	6,881.7	4,423.9	3,307.4	5,787.0	25	4,575.7	8,042.6	6,188.9	4,891.9	7,352.9	21
OA 0 yr	3,345.7	6,274.1	4,387.2	3,665.2	5,161.0	47	4,589.7	8,523.4	6,725.7	5,610.9	7,752.4	43
OA 1.5 yr	3,359.3	5,958.5	4,406.3	3,682.6	5,109.7	42	4,605.5	8,660.8	6,786.8	5,713.6	7,780.3	42
OA 3 yr	3,366.6	6,289.7	4,429.6	3,686.3	5,140.2	42	4,771.6	8,719.3	6,799.3	5,766.8	7,877.3	39

Table IV

Minimum, maximum, median, 5th percentile, and 75th percentile of osteophyte volume (OP) (mm³) of the trapezium (TPM) and first metacarpal (MC1). The values listed for the non-OA are those of the healthy reference library and represent volumes associated with variations in bone shapes across that cohort

Women						Men						
TPM	min	max	median	25 th %	75 th %	n	min	max	median	25 th %	75 th %	n
non-OA	36.8	117.2	59.2	39.3	92.6	25	60.6	163.5	109.1	69.3	136.7	21
OA 0 yr	38.5	414.9	79.7	21.2	176.7	47	59.9	802.5	163.3	25.2	364.9	43
OA 1.5 yr	36.3	279.9	100.4	35.5	210.9	42	58.2	719.5	187.0	61.6	383.1	42
OA 3 yr	46.0	357.8	108.4	35.0	239.1	42	62.7	764.4	236.0	65.3	461.3	39
MC1	min	max	median	25 th %	75 th %	n	min	max	median	25 th %	75 th %	n
non-OA	6.3	116.1	43.2	16.6	82.3	25	34.3	224.2	72.2	29.2	138.6	21
OA 0 yr	10.6	381.4	59.0	4.7	155.5	47	29.2	560.5	119.7	24.1	260.7	43
OA 1.5 yr	4.7	402.8	79.1	7.3	195.3	42	20.9	607.7	149.3	35.5	309.1	42
OA 3 yr	6.6	400.1	83.7	9.5	201.1	42	13.7	460.6	176.8	54.8	335.0	39

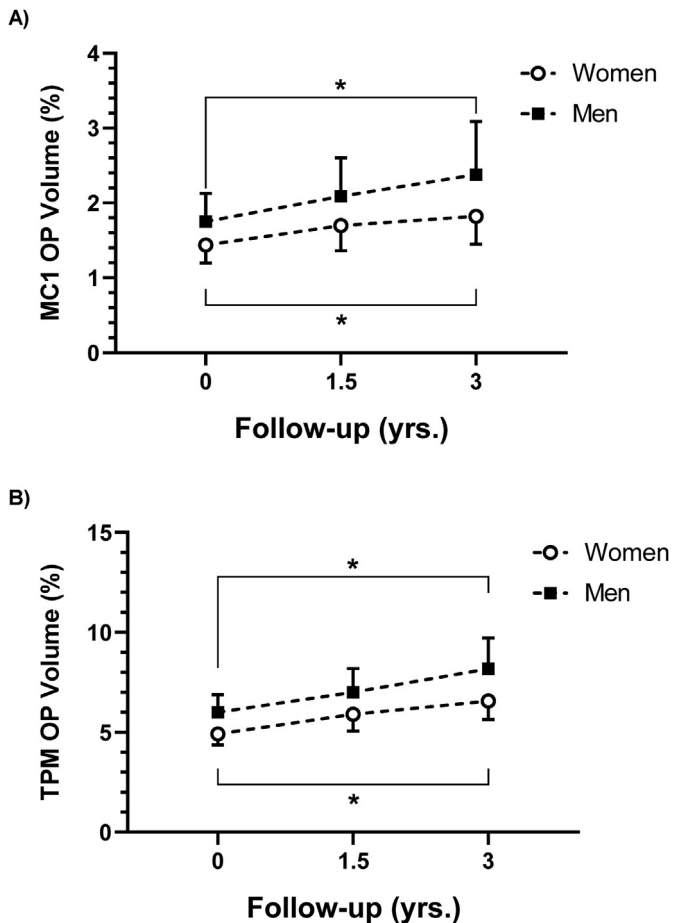


Fig. 3. Osteophyte volume (OP) as a percentage of total bone volume increased significantly in women and men over the three-year follow up in the MC1 (A) and TPM (B). While men tended to have larger normalized OP than women at all time points, the differences were not statistically significant. Model-based means and with their 95% CIs are plotted.

($\geq 17\%$) in the thumb CMC joint, and osteophytes on the radial and ulnar margins of the trapezia. Buckland-Wright's findings differ from ours in that they identified osteophytes on the radial and ulnar margins of the MC1, and they did not see significant progression over the 18-month duration of their study. Buckland-Wright *et al.* studied patients with long-standing disease (mean duration 11.6 ± 10 yrs), while we specifically recruited patients with early-stage disease, and this is likely one contributing factor to the differences in the findings. A potentially larger factor that remains to be more thoroughly examined is the correlation, or lack thereof, in defining osteophyte size and location on radiographs as opposed to 3D reconstructions from CT images.

The fact that osteophytes first form in consistent, non-opposing regions of the trapezium and MC1 is intriguing (Fig. 4). Identifying the mechanism behind this could advance our understanding of the etiology and progression of OA. Potential mechanisms include altered mechanical stress at ligament and/or capsular insertions, altered contact stress, or variation in responsive cell populations. The stabilizing ligamentous structures of the CMC joint have been described^{48–51}. The volar ligaments include the superficial and deep anterior oblique ligaments (AOL) and the ulnar collateral ligament. The dorsal ligaments include the dorsal trapeziometacarpal ligament, posterior oblique ligament, dorsal central ligament, and the dorsal radial ligament (DRL). The DRL originates from the dorsoradial tubercle of the trapezium and

inserts on the dorsal edge of the first metacarpal base⁴⁸. It is the widest, thickest, and shortest of the stabilizing ligaments, and thus postulated to play an important role in joint stabilization⁴⁸ as it also sustained the greatest ultimate load⁵⁰. While there has been debate, the dorsal ligaments are now generally believed to act as the primary restraints to several movements^{51–53}, including posterior shear, translation, and dislocation, with the volar AOL ligament serving as a thin tension band to support the dorsal restraints⁵⁴. Regardless of the stabilizing role assigned to the ligaments, we postulate that they are the least likely explanation of the patterned growth because the insertion sites generally oppose one another across the CMC joint, which is not consistent with our observation of osteophyte growth at non-opposing locations.

On the TPM and MC1, osteophytes formed in regions with similar bony topology – at the margins of the apices of the concave portions of the articular surfaces. This was first described by North and Rutledge²². We would describe these locations as having high convex curvature relative to the margins of the articular facets. Considering that stresses are developed in bones during activities, it is possible that the stresses developed in these bone regions yield higher bone strains than the concave regions of the rims of the articular facet, given their unique shape and location. If so, this would suggest an intriguing mechanism for osteophyte formation. A more detailed analysis, such as finite element modeling, could potentially shed light on the likelihood of this mechanism.

The net effect of non-opposing osteophyte formation, which exaggerates the normal saddle joint contour, may also result in a greater constraint of overall joint motion and increased mechanical stability of the joint itself. This could conceivably be answered with a well-designed cadaver study. It is also possible that osteophytes develop in specific areas due to differences in cell populations or tissue responsiveness to loading, but we have been unable to locate any information that details cell type by locations in these bones.

The rate of osteophyte growth increased with time (Fig. 3). At year 3, OP was approximately 6.4% and 8.2% of total TPM volume and 1.8% and 2.4% of the MC1 in women and men, respectively. While these values are a relatively small percentage of total bone volume, osteophyte growth was localized so the dimensions of the osteophytes at year three were typically in the range of a millimeter or greater. This is generally consistent with radiographically moderate (Stage II–III/Stage 2–3) thumb CMC OA²³. Mean OPs tended to be larger in men than women, even after normalizing for the effects of bone size. This is surprising, given that the prevalence of thumb CMC OA is greater in women than men^{25,55–57} in some reports by a ratio of $\sim 2:1$ ^{25,26}. It is also possible that this trend is simply an artifact of our sample populations since men were on average seven years older than the women. Additional studies will be needed to confirm (or refute) this observation.

When interpreting our findings, it should be noted that this study focused on reporting the growth and location of osteophytes only about the thumb CMC joint. We did not examine changes at the two other joints of the trapezium nor the distal joint of the first metacarpal. In our initial data analysis, we noted changes across the entire surface of both bones, therefore we truncated our bone models with cross-sectioning planes (Fig. 1(B)) to focus this study on the CMC joint. Schneider *et al.* used time 0 image data from a subset of our study subjects to characterize morphological changes via statistical shape modeling³². They found that the trapezia and first metacarpals in early OA patients were shorter and wider than healthy controls, and that their articular surfaces were wider and deeper. The morphological changes across the entire bones that may occur with disease progression remain to be examined.

The chief limitation of this study is that we did not have an age- and sex-matched group of healthy controls for comparison with our OA cohort, so we cannot definitively rule out the possibility that the

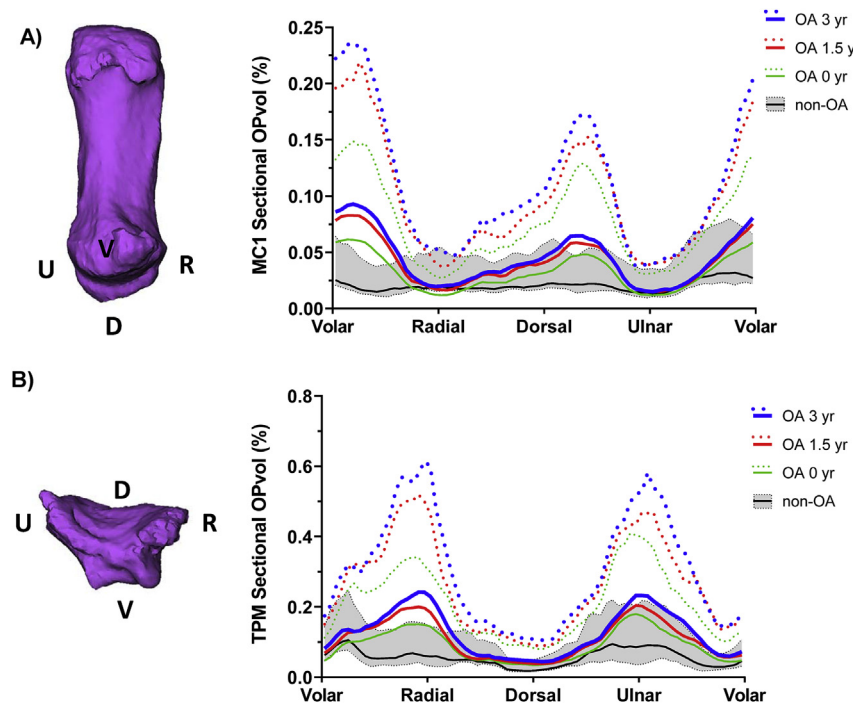


Fig. 4. Osteophyte growth on the first metacarpal (MC1) (A) and on the trapezium (TPM) (B) progressed in non-opposing locations from 0 to 1.5–3 yrs. Osteophytes are described by their volume within 5° sections (Sectional OPvol) about each respective facet, normalized by total bone volume (%), and plotted as a function of location within a 360° arc. Locations are labeled by anatomical direction (volar (V), radial (R), dorsal (D), and ulnar (U)). The median (solid lines) and 75th percentile (dotted lines) sectional osteophyte volumes for the early OA cohort, pooled across men and women, are plotted for each follow-up time point. The median (solid line), 25th percentile, and 75th percentile (gray band) curves of the non-OA represent the volume of bone associated with shape variations within the reference library.

changes we documented were associated with aging as opposed to osteoarthritis. However, when viewed in the context of the numerous animal and human studies that have examined osteophytes in OA, we think it is most likely that the bony changes we measured reflect OA progression^{16,58–60}. A second limitation is that our Boolean subtraction approach to quantifying bone changes cannot automatically differentiate bone shape from minor osteophytes. However, we do not consider this insurmountable because the bone changes seen in the non-OA cohort are substantially smaller than those computed for the patients with early OA (refer to non-OAs in Table IV). Finally, factors confounding or correlating with osteophyte formation were not examined. Studies in animals and humans have reported that increased osteophyte formation is associated with decreased joint ROM and increased joint stability^{15,21}. Joint space narrowing has also been associated with osteophyte formation⁴. In the thumb CMC joint, the saddle-shaped geometry of the healthy joint and the subsequent changes in the shape of the joint space with OA progression²⁴ can confound the calculation of joint space narrowing. Future analyses will be needed to examine these relations with osteophyte growth at the CMC joint.

Author contributions

- Conception and design – JJC, AMM, DCM, ALL, APCW
- Analysis and interpretation of the data – JJC, AMM, DCM, ALL, APCW
- Drafting of the article – JJC, AMM, DCM, LGK
- Critical revision of the article for important intellectual content – All authors
- Final approval of the article – All authors
- Obtaining of funding – JJC, DCM, ALL, APCW
- Collection and assembly of data – JJC, AMM, DCM, ALL, APCW

Conflict of interest

We declare no conflict of interests.

Funding sources

Research reported in this publication was supported by the National Institute of Arthritis and Musculoskeletal and Skin Diseases of the National Institutes of Health under Award Number R01 AR059185. The content is solely the responsibility of the authors and does not necessarily represent the official views of the National Institutes of Health.

References

1. Eaton RG, Littler JW. Ligament reconstruction for the painful thumb carpometacarpal joint. *J Bone Joint Surg Am* 1973;55(8):1655–66.
2. Eaton RG, Glickel SZ. Trapeziometacarpal osteoarthritis. Staging as a rationale for treatment. *Hand Clin* 1987;3(4):455–71.
3. Ladd AL, Messana JM, Berger AJ, Weiss A-PC. Correlation of clinical disease severity to radiographic thumb osteoarthritis index. *J Hand Surg Am* 2015;40(3):474–82, <https://doi.org/10.1016/j.jhsa.2014.11.021>.
4. Cicuttini FM, Baker J, Hart DJ, Spector TD. Association of pain with radiological changes in different compartments and views of the knee joint. *Osteoarthritis Cartilage* 1996;4(2):143–7.
5. Kamimura M. Joint pain undergoes a transition in accordance with signal changes of bones detected by MRI in hip osteoarthritis. *Open Rheumatol J* 2013;7(1):67–74, <https://doi.org/10.2174/1874312920130823002>.
6. Kroon FPB, van Beest S, Ermurat S, Kortekaas MC, Bloem JL, Reijnierse M, et al. In thumb base osteoarthritis structural damage is more strongly associated with pain than synovitis.

Osteoarthritis Cartilage 2018;26(9):1196–202, <https://doi.org/10.1016/j.joca.2018.04.009>.

7. Kato H. Knee joint pain potentially due to bone alterations in a knee osteoarthritis patient. American Journal of Case Reports 2014;15:534–7, <https://doi.org/10.12659/AJCR.891233>.
8. Komatsu M, Kamimura M, Nakamura Y, Mukaiyama K, Ikegami S, Hayashi M, et al. Bony findings detected by MRI may reflect the pathophysiology of osteoarthritis with thumb carpometacarpal joint pain. Int J Rheum Dis 2017;20(12):1950–7, <https://doi.org/10.1111/1756-185X.12781>.
9. Kamimura M, Nakamura Y, Uchiyama S, Ikegami S, Mukaiyama K, Kato H. The pathophysiology and progression of hip osteoarthritis accompanied with joint pain are potentially due to bone alterations - follow-up study of hip OA patients. Open Rheumatol J 2014;8:46–53, <https://doi.org/10.2174/1874312901408010046>.
10. Moskowitz RW, Goldberg VM. Osteophyte evolution: studies in an experimental partial meniscectomy model. J Rheumatol 1987;14:116–8.
11. van der Kraan PM, van den Berg WB. Osteophytes: relevance and biology. Osteoarthritis Cartilage 2007;15(3):237–44, <https://doi.org/10.1016/j.joca.2006.11.006>.
12. Menkes CJ, Lane NE. Are osteophytes good or bad? Osteoarthritis Cartilage 2004;12(Suppl A):S53–4.
13. Wong SHJ, Chiu KY, Yan CH. Review article: osteophytes. J Orthop Surg 2016;24(3):403–10, <https://doi.org/10.1177/1602400327>.
14. Nagaosa Y, Lanyon P, Doherty M. Characterisation of size and direction of osteophyte in knee osteoarthritis: a radiographic study. Ann Rheum Dis 2002;61(4):319–24, <https://doi.org/10.1136/ard.61.4.319>.
15. Pottenger LA, Phillips FM, Draganich LF. The effect of marginal osteophytes on reduction of varus-valgus instability in osteoarthritic knees. Arthritis Rheum 1990;33(6):853–8.
16. Felson DT, Gale DR, Elon Gale M, Niu J, Hunter DJ, Goggins J, et al. Osteophytes and progression of knee osteoarthritis. Rheumatology 2005;44(1):100–4, <https://doi.org/10.1093/rheumatology/keh411>.
17. Uchino M, Izumi T, Tominaga T, Wakita R, Minehara H, Sekiguchi M, et al. Growth factor expression in the osteophytes of the human femoral head in osteoarthritis. Clin Orthop Relat Res 2000;377:119–25.
18. van Beuningen HM, Glansbeek HL, van der Kraan PM, van den Berg WB. Osteoarthritis-like changes in the murine knee joint resulting from intra-articular transforming growth factor-beta injections. Osteoarthritis Cartilage 2000;8(1):25–33, <https://doi.org/10.1053/joca.1999.0267>.
19. Brandt KD. Osteophytes in osteoarthritis. Clinical aspects. Osteoarthritis Cartilage 1999;7(3):334–5, <https://doi.org/10.1053/joca.1998.0187>.
20. Ritter MA, Harty LD, Davis KE, Meding JB, Berend ME. Predicting range of motion after total knee arthroplasty. Clustering, log-linear regression, and regression tree analysis. J Bone Joint Surg Am 2003;85-A(7):1278–85.
21. Hsia AW, Anderson MJ, Heffner MA, Lagmay EP, Zavodovskaya R, Christiansen BA. Osteophyte formation after ACL rupture in mice is associated with joint restabilization and loss of range of motion. J Orthop Res 2017;35(3):466–73, <https://doi.org/10.1002/jor.23252>.
22. North ER, Rutledge WM. The trapezium-thumb metacarpal joint: the relationship of joint shape and degenerative joint disease. Hand 1983;15(2):201–6.
23. Pellegrini VD. Osteoarthritis of the trapeziometacarpal joint: the pathophysiology of articular cartilage degeneration. I. Anatomy and pathology of the aging joint. J Hand Surg 1991;16(6):967–74, [https://doi.org/10.1016/S0363-5023\(10\)80054-1](https://doi.org/10.1016/S0363-5023(10)80054-1).
24. Van Nortwick S, Berger A, Cheng R, Lee J, Ladd AL. Trapezial topography in thumb carpometacarpal arthritis. J Wrist Surg 2013;2(3):263–70, <https://doi.org/10.1055/s-0033-1350088>.
25. Dahaghin S, Bierma-Zeinstra SMA, Ginai AZ, Pols HAP, Hazes JMW, Koes BW. Prevalence and pattern of radiographic hand osteoarthritis and association with pain and disability (the Rotterdam study). Ann Rheum Dis 2005;64(5):682–7, <https://doi.org/10.1136/ard.2004.023564>.
26. Sodha S, Ring D, Zurakowski D, Jupiter JB. Prevalence of osteoarthritis of the trapeziometacarpal joint. J Bone Joint Surg Am 2005;87(12):2614–8, <https://doi.org/10.2106/JBJS.E.00104>.
27. Crisco JJ, Halilaj E, Moore DC, Patel T, Weiss A-PC, Ladd AL. In Vivo kinematics of the trapeziometacarpal joint during thumb extension-flexion and abduction-adduction. J Hand Surg Am 2015;40(2):289–96, <https://doi.org/10.1016/j.jhsa.2014.10.062>.
28. Halilaj E, Rainbow MJ, Got C, Schwartz JB, Moore DC, Weiss A-PC, et al. In vivo kinematics of the thumb carpometacarpal joint during three isometric functional tasks. Clin Orthop Relat Res 2014;472(4):1114–22, <https://doi.org/10.1007/s11999-013-3063-y>.
29. Halilaj E, Moore DC, Patel TK, Laidlaw DH, Ladd AL, Weiss A-PC, et al. Older asymptomatic women exhibit patterns of thumb carpometacarpal joint space narrowing that precede changes associated with early osteoarthritis. J Biomech 2015;48(13):3643–9, <https://doi.org/10.1016/j.jbiomech.2015.08.010>.
30. Crisco JJ, Patel T, Halilaj E, Moore DC. The envelope of physiological motion of the first carpometacarpal joint. J Biomech Eng 2015;137(10):101002, <https://doi.org/10.1115/1.4031117>.
31. Halilaj E, Laidlaw DH, Moore DC, Crisco JJ. How do sex, age, and osteoarthritis affect cartilage thickness at the thumb carpometacarpal joint? Insights from subject-specific cartilage modeling. In: Tavares JMRS, Luo X, Li S, Eds. Bio-Imaging And Visualization for Patient-Customized Simulations. Lecture Notes in Computational Vision and Biomechanics. Cham, Switzerland: Springer International Publishing; 2014:103–11, https://doi.org/10.1007/978-3-319-03590-1_9.
32. Schneider MTY, Zhang J, Walker CG, Crisco JJ, Weiss A-PC, Ladd AL, et al. Early morphologic changes in trapeziometacarpal joint bones with osteoarthritis. Osteoarthritis Cartilage 2018;26(10):1338–44, <https://doi.org/10.1016/j.joca.2018.06.008>.
33. McQuillan TJ, Kenney D, Crisco JJ, Weiss A-P, Ladd AL. Weaker functional pinch strength is associated with early thumb carpometacarpal osteoarthritis. Clin Orthop Relat Res 2016;474(2):557–61, <https://doi.org/10.1007/s11999-015-4599-9>.
34. Halilaj E, Rainbow MJ, Got CJ, Moore DC, Crisco JJ. A thumb carpometacarpal joint coordinate system based on articular surface geometry. J Biomech 2013;46(5):1031–4, <https://doi.org/10.1016/j.jbiomech.2012.12.002>.
35. Halilaj E, Moore DC, Patel TK, Ladd AL, Weiss A-PC, Crisco JJ. Early osteoarthritis of the trapeziometacarpal joint is not associated with joint instability during typical isometric loading. J Orthop Res 2015;33(11):1639–45, <https://doi.org/10.1002/jor.22936>.
36. McQuillan TJ, Vora MM, Kenney DE, Crisco JJ, Weiss A-PC, Ebert KA, et al. The AUSCAN and PRWHE demonstrate comparable internal consistency and validity in patients with early thumb carpometacarpal osteoarthritis. Hand (N Y) 2018;13(6):652–8, <https://doi.org/10.1177/1558944717729217>.
37. Halilaj E, Moore DC, Patel TK, Ladd AL, Weiss A-PC, Crisco JJ. Early osteoarthritis of the trapeziometacarpal joint is not

associated with joint instability during typical isometric loading. *J Orthop Res* 2015;33(11):1639–45, <https://doi.org/10.1002/jor.22936>.

38. Biswas D, Bible JE, Bohan M, Simpson AK, Whang PG, Grauer JN. Radiation exposure from musculoskeletal computerized tomographic scans. *J Bone Joint Surg Am* 2009;91(8):1882–9, <https://doi.org/10.2106/JBJS.H.01199>.
39. Manu. nonrigidICP. MATLAB central file exchange. <https://www.mathworks.com/matlabcentral/fileexchange/41396-nonrigidicp>. Published 2019. Accessed March 1, 2019.
40. Claes P, Daniels K, Walters M, Clement J, Vandermeulen D, Suetens P. Dysmorphometrics: the modelling of morphological abnormalities. *Theor Biol Med Model* 2012;9:5, <https://doi.org/10.1186/1742-4682-9-5>.
41. Morton A. An Approach to Quantifying Osteophyte Formation with OA Progression of the Thumb Carpometacarpal Joint. Unpublished study.
42. Van Haver A, Mahieu P, Claessens T, Li H, Pattyn C, Verdonk P, et al. A statistical shape model of trochlear dysplasia of the knee. *The Knee* 2014;21(2):518–23, <https://doi.org/10.1016/j.knee.2013.11.016>.
43. Oura K, Moritomo H, Kataoka T, Oka K, Murase T, Sugamoto K, et al. Three-dimensional analysis of osteophyte formation on distal radius following scaphoid nonunion. *J Orthop Sci* 2017;22(1):50–5, <https://doi.org/10.1016/j.jtos.2016.06.018>.
44. Eberly D, Lancaster J, Alyassin A. On gray scale image measurements: II. Surface area and volume. *CVGIP Graph Models Image Process* 1991;53(6):550–62, [https://doi.org/10.1016/1049-9652\(91\)90005-5](https://doi.org/10.1016/1049-9652(91)90005-5).
45. Schneider MTY, Zhang J, Crisco JJ, Weiss APC, Ladd AL, Nielsen P, et al. Men and women have similarly shaped carpometacarpal joint bones. *J Biomech* 2015;48(12):3420–6, <https://doi.org/10.1016/j.jbiomech.2015.05.031>.
46. Crisco JJ, Coburn JC, Moore DC, Upal MA. Carpal bone size and scaling in men versus in women. *J Hand Surg Am* 2005;30(1):35–42, <https://doi.org/10.1016/j.jhsa.2004.08.012>.
47. Buckland-Wright JC, Macfarlane DG, Lynch JA. Osteophytes in the osteoarthritic hand: their incidence, size, distribution, and progression. *Ann Rheum Dis* 1991;50(9):627–30.
48. Bettinger PC, Linscheid RL, Berger RA, Cooney WP, An KN. An anatomic study of the stabilizing ligaments of the trapezium and trapeziometacarpal joint. *J Hand Surg [Am]* 1999;24:786–98.
49. Pellegrini VD. Pathomechanics of the thumb trapeziometacarpal joint. *Hand Clin* 2001;17:175–84. vii–viii.
50. Bettinger PC, Berger RA. Functional ligamentous anatomy of the trapezium and trapeziometacarpal joint (gross and arthroscopic). *Hand Clin* 2001;17(2):151–68. vii.
51. Ladd AL, Lee J, Hagert E. Macroscopic and microscopic analysis of the thumb carpometacarpal ligaments: a cadaveric study of ligament anatomy and histology. *J Bone Jt Surg* 2012;94(16):1468–77, <https://doi.org/10.2106/JBJS.K.00329>.
52. Hagert E, Lee J, Ladd AL. Innervation patterns of thumb trapeziometacarpal joint ligaments. *J Hand Surg Am* 2012;37(4):706–14, <https://doi.org/10.1016/j.jhsa.2011.12.038>. e1.
53. Halilaj E, Rainbow MJ, Moore DC, Laidlaw DH, Weiss A-PC, Ladd AL, et al. In vivo recruitment patterns in the anterior oblique and dorsoradial ligaments of the first carpometacarpal joint. *J Biomech* 2015;48(10):1893–8, <https://doi.org/10.1016/j.jbiomech.2015.04.028>.
54. Zhang AY, Van Nortwick S, Hagert E, Yao J, Ladd AL. Thumb carpometacarpal ligaments inside and out: a comparative study of arthroscopic and gross anatomy from the Robert A. Chase hand and upper limb center at Stanford University. *J Wrist Surg* 2013;2(1):55–62, <https://doi.org/10.1055/s-0033-1333683>.
55. Haara MM, Heliövaara M, Kröger H, Arokoski JPA, Manninen P, Kärkkäinen A, et al. Osteoarthritis in the carpometacarpal joint of the thumb. Prevalence and associations with disability and mortality. *J Bone Joint Surg Am* 2004;86-A(7):1452–7.
56. Kellgren JH, Lawrence JS. Osteoarthritis and disk degeneration in an urban population. *Ann Rheum Dis* 1958;17(4):388–97.
57. Haugen IK, Englund M, Aliabadi P, Niu J, Clancy M, Kvien TK, et al. Prevalence, incidence and progression of hand osteoarthritis in the general population: the Framingham Osteoarthritis Study. *Ann Rheum Dis* 2011;70(9):1581–6, <https://doi.org/10.1136/ard.2011.150078>.
58. Turmezei TD, Poole KES. Computed tomography of subchondral bone and osteophytes in hip osteoarthritis: the shape of things to come? *Front Endocrinol* 2011;2, <https://doi.org/10.3389/fendo.2011.00097>.
59. Bechtold TE, Saunders C, Decker RS, Um H-B, Cottingham N, Salhab I, et al. Osteophyte formation and matrix mineralization in a TMJ osteoarthritis mouse model are associated with ectopic hedgehog signaling. *Matrix Biol* 2016;52–54:339–54, <https://doi.org/10.1016/j.matbio.2016.03.001>.
60. Junker S, Krumbholz G, Frommer KW, Rehart S, Steinmeyer J, Rickert M, et al. Differentiation of osteophyte types in osteoarthritis – proposal of a histological classification. *Jt Bone Spine* 2016;83(1):63–7, <https://doi.org/10.1016/j.jbspin.2015.04.008>.